

## SEGREGATION OF SOLUTES IN TWO-PHASE MIXTURES

Matthew O. Zacate, Bonner C. Walsh, Luke S.-J. Peng, and Gary S. Collins

*Department of Physics, Washington State University, Pullman, WA 99164, USA*

Fractions of indium solutes in each phase of a mixture of two binary phases were measured using perturbed angular correlation of gamma rays. Measurements of phase fractions were made on Pd<sub>3</sub>Ga<sub>7</sub>-PdGa, PdGa-Pd<sub>5</sub>Ga<sub>3</sub>, and FeAl<sub>2</sub>-FeAl mixtures as a function of composition. The phase fractions were analyzed using a thermodynamic model that takes into account differences between energies of solute atoms in the two phases. From the model, segregation coefficients were obtained for the systems studied. Also, earlier measurements on Ni<sub>2</sub>Al<sub>3</sub>-NiAl were reanalyzed. Large differences are found among the segregation coefficients.

The volume fractions of phases in a mixture of two phases are given by the lever rule. A solute in the mixture will partition itself between the two phases, but the fraction of solute in each phase (called solute phase fraction below) will not in general equal the volume fraction. One way to measure solute phase fractions is through hyperfine interactions of impurity probes. When hyperfine interactions in the two phases differ, the ratio of signal amplitudes is equal to the ratio of solute phase fractions. The ratio of solute phase fractions,  $f_1/f_2$ , is related to the ratio of volume fractions,  $(x_2-x)/(x-x_1)$ , via [1,2]

$$\frac{f_1}{f_2} = \frac{1}{A} \left( \frac{x_2 - x}{x - x_1} \right) \exp \left( \frac{G_2 - G_1}{k_B T} \right), \quad (1)$$

in which  $x$  is the sample composition,  $x_1$  is the boundary composition between phase 1 and the two-phase field,  $x_2$  is the boundary between phase 2 and the two-phase field,  $A$  is the ratio of fractions of crystallographic sites occupied by solute atoms in the two phases,  $G_1$  and  $G_2$  are changes in Gibbs free energies when the solute is incorporated in each phase,  $k_B$  is the Boltzmann constant, and  $T$  is absolute temperature. If  $A=1$  and  $\Delta G=0$ , solute phase fractions reduce to the volume fractions. In general,  $A \neq 1$ ; for example, if phases 1 and 2 are stoichiometric NiAl and Ni<sub>3</sub>Al and the solute is located solely on Ni-sublattices, then factor  $A=(3/4)/(1/2)=3/2$ . Preference of a solute for a phase occurs when  $\Delta G \neq 0$  and will be termed segregation. It is convenient to define a segregation coefficient  $C_{seg} \equiv \exp((G_2 - G_1)/k_B T)$ . When  $C_{seg}$  is greater than unity, solutes prefer to occupy sites in phase 1, leading to an enhancement of the solute fraction in phase 1.

Perturbed angular correlation of gamma rays (PAC) has been used to measure fractions of indium solute in each phase of the mixtures Ni<sub>2</sub>Al<sub>3</sub>-NiAl [1,2], Pd<sub>3</sub>Ga<sub>7</sub>-PdGa [3], PdGa-Pd<sub>5</sub>Ga<sub>3</sub> [3], and FeAl<sub>2</sub>-FeAl [4]. The phases will have the compositions of the boundaries of the two-phase field ( $x_1$  and  $x_2$ ). Accordingly, phase fractions will depend on the composition of the mixture ( $x$ ) while the hyperfine interactions will not. In the present paper, measured solute phase fractions are analyzed with results expressed in terms of  $C_{seg}$ . Samples were prepared by arc-melting high purity metal foils with <sup>111</sup>In (fractional concentration  $\sim 10^{-8}$ ). Samples were then annealed to coarsen grains, remove lattice defects, and establish an equilibrium distribution of solute between the two phases. After annealing and prior to measurement, samples were cooled to room temperature over 5-10 hours. Details of sample preparation are given elsewhere [1,2,3]. Nominal sample compositions were determined by masses of the starting foils. Small mass losses during arc-melting were assumed to be caused by evaporation of the more volatile element, leading to minor adjustments in the assumed composition. PAC measurements were made using a standard 4-detector PAC spectrometer [5]. Spectra for Pd-Ga were corrected for an offset due to correlated source self-absorption

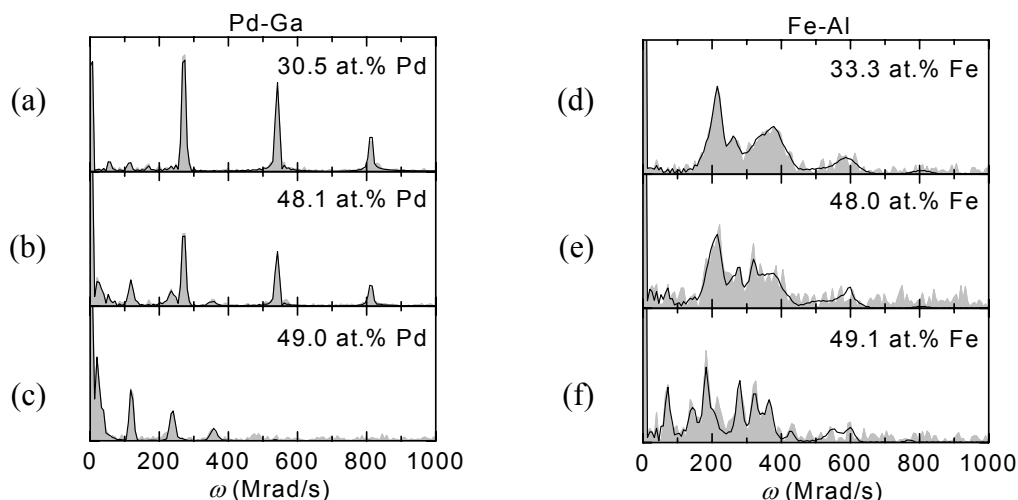


Figure 1. Fourier amplitude transforms of PAC spectra of Pd-Ga and Fe-Al systems at room temperature. Shown are (a) Pd<sub>3</sub>Ga<sub>7</sub> (30.5 at.% Pd), (b) Pd-Ga 48.1 at.% Pd, (c) PdGa (49.0 at.% Pd), (d) FeAl<sub>2</sub> (33.3 at.% Fe), (e) Fe-Al 48.0 at.% Fe, and (f) Fe-Al (49.1 at.% Fe).

[6]. PAC spectra for Ni-Al were shown previously in refs. [1,2]. Fourier amplitude transforms of representative spectra for the Pd-Ga and Fe-Al systems are shown in Fig. 1 together with results of computer fits.

Pd-Ga phase mixtures. Indium solutes will be assumed below to only occupy Ga-sites in the two phases. Pd<sub>3</sub>Ga<sub>7</sub> has the Ir<sub>3</sub>Ge<sub>7</sub> structure, which contains two inequivalent Ge-sites, Ge(1) and Ge(2), respectively with 3 and 4 sites per unit cell and  $\bar{4}m.2$  and  $.3m$  site symmetries. If indium substitutes randomly on both Ge-sites, one will measure two axially symmetric quadrupole interaction signals with site-fractions in proportion to 3:4. To identify site(s) occupied by indium in Pd<sub>3</sub>Ga<sub>7</sub>, measurements were made on isostructural Pt<sub>3</sub>In<sub>7</sub>. In agreement with prior measurements on Pt<sub>3</sub>In<sub>7</sub> made by M. Marszalek et al. [7], two axially symmetric signals were observed with fundamental measured frequencies  $\omega_1=301.9(1)$  Mrad/s and  $\omega_2=87.4(1)$  Mrad/s and site-fractions in a ratio close to 3:4, identifying the sites respectively as In(1) and In(2), in analogy with sites Ge(1) and Ge(2). In Pd<sub>3</sub>Ga<sub>7</sub>, one predominant axially symmetric signal was observed with a frequency of 267 Mrad/s that is much closer to the 301.9 Mrad/s frequency of the In(1) site than the 87.4 Mrad/s signal of the In(2) site. We therefore attribute the 267 Mrad/s signal to In on the Ga(1) site (denoted In<sub>Ga</sub>(1)). A small amount of a 59 Mrad/s signal was also observed that is attributed to In<sub>Ga</sub>(2). The In<sub>Ga</sub>(1) signal has a site fraction that is 20-40 times larger than that of In<sub>Ga</sub>(2), indicating that indium substitutes preferentially at the Ga(1) site. Similar strong site substitution preference has been observed in Ni<sub>2</sub>Al<sub>3</sub> [8] and bixbyite [9] structures. Signals observed and site attributions are summarized in Table 1.

PdGa has the FeSi structure, in which there is a unique Ga-site with  $.3$  site symmetry. Probes substituting for Ga can therefore be expected to exhibit an axially symmetric efg. A predominant axially-symmetric signal was observed at the stoichiometric composition that is attributed to the Ga-site (signal 5 in table 1). In addition, other signals whose site fractions vary with composition were observed in Pd-poor PdGa (signals 6-8). These are attributed to indium probes on Ga sites with defects in near-neighbor positions or, possibly, on Pd sites.

Table 1  
 Hyperfine parameters of PAC signals observed in spectra of  $\text{Pt}_3\text{In}_7$ ,  $\text{Pd}_3\text{Ga}_7$ , and  $\text{PdGa}$  systems.

phase	signal no.	$\omega_1$ (Mrad/s)	$\eta$	Site attribution
$\text{Pt}_3\text{In}_7$	1	301.9(1)	0	In(1)
	2	87.4(1)	0	In(2)
$\text{Pd}_3\text{Ga}_7$	3	267(1)	0	$\text{In}_{\text{Ga}(1)}$
	4	59(5)	0	$\text{In}_{\text{Ga}(2)}$
$\text{PdGa}$	5	117(1)	0	$\text{In}_{\text{Ga}}$
	6	20(2)	0.4(1)	$\text{In}_{\text{Pd}}$ or $\text{In}_{\text{Ga}}$ +defect (1)
	7	12(1)	0	$\text{In}_{\text{Pd}}$ or $\text{In}_{\text{Ga}}$ +defect (2)
	8	22(5)	0.8 <sub>4</sub> (2)	$\text{In}_{\text{Pd}}$ or $\text{In}_{\text{Ga}}$ +defect (3)

All spectra for the Pd-Ga system exhibited an unperturbed signal with a site fraction of order 10% that had no clear dependence on composition. As a consequence, the unperturbed signal was not assigned to either the  $\text{Pd}_3\text{Ga}_7$  or  $\text{PdGa}$  phases in the analysis of indium segregation. Hence, the  $\text{Pd}_3\text{Ga}_7$  phase fraction was determined by summing site fractions of signals 3 and 4, and the  $\text{PdGa}$  phase fraction by summing site fractions of signals 5-8. The two phase fractions were then normalized so their sum was unity, and are plotted as a function of composition between 30 and 50 at.% Pd in Fig. 2(a). Curves in the figure show results of fitting the  $\text{Pd}_3\text{Ga}_7$  phase fraction ( $f_1$ ) using eq. 1 with the normalization condition:  $f_2 = 1 - f_1$ . In the fits, the  $\text{Pd}_3\text{Ga}_7$  boundary was taken to be at 30.0 at.% Pd and the  $\text{PdGa}$  boundary at 49.3 at.% Pd based on a consideration of the PAC data and published phase boundaries. The ratio  $A$  used in the fitting was 5/3, based on the observation that In appears to substitute exclusively on site Ga(1). The result is  $C_{\text{seg}}=45(7)$ . Similar measurements and analysis carried out for the phase 1-2 mixture  $\text{PdGa}$ - $\text{Pd}_5\text{Ga}_3$  yield  $C_{\text{seg}}=0.6(2)$  [3].

Fe-Al phase mixtures.  $\text{FeAl}_2$  is a disordered monoclinic compound containing 13 inequivalent, partially filled sites for Al and 8 partially filled sites for Fe. Thus, one expects a plethora of non-axially symmetric PAC signals from indium substituting at various sites in the structure as well as inhomogeneity due to lattice disorder. To provide an fingerprint of the  $\text{FeAl}_2$  phase, the PAC spectrum for the 33.3 at.% Fe sample was fitted empirically using four broadened signals, yielding hyperfine parameters and relative fractions listed in Table 2.

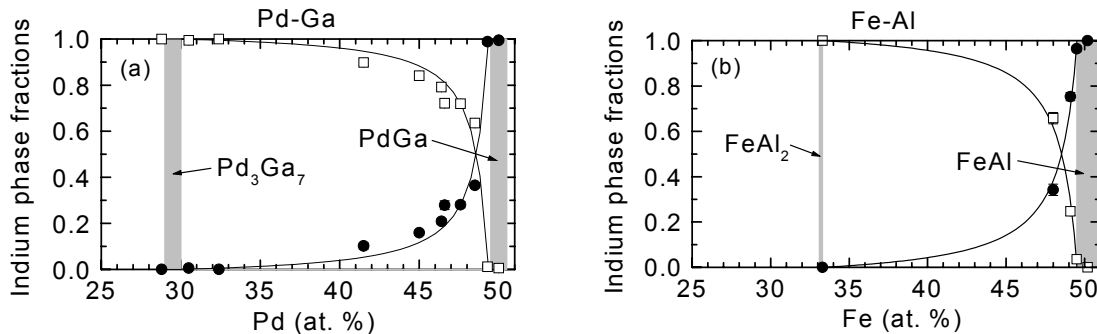


Figure 2. Indium solute phase fractions in (a) the Pd-Ga system and in (b) the Fe-Al system. Squares indicate fractions of probes in (a)  $\text{Pd}_3\text{Ga}_7$  or (b)  $\text{FeAl}_2$ . Circles indicate fractions of probes in (a)  $\text{PdGa}$  or (b)  $\text{FeAl}$ . Curves drawn are from fits of the data using eq. 1. Shaded regions indicate extents of single-phase fields.

Table 2  
 Hyperfine interaction parameters of PAC signals fitted to the FeAl<sub>2</sub> spectrum.

signal no.	signal fraction (%)	$\omega_1$ (Mrad/s)	$\eta$
1	39.2(4)	214(1)	0.37(2)
2	27.2(4)	192(6)	0.47(4)
3	19.9(2)	258(2)	0.70(2)
4	13.7(1)	386(4)	0.92(1)

FeAl has the CsCl structure and a large amount of quenched-in disorder [10]. Seven PAC signals have been observed in FeAl, five associated with non-cubic configurations of vacancies in the first neighbor shell of indium solutes (see ref. [10]), one with a frequency of 22 Mrad/s attributed to an Fe<sub>Al</sub> antisite defect in the second neighbor shell, and a defect-free signal with zero frequency. In the two-phase field between FeAl<sub>2</sub> and FeAl, site fractions of all eleven signals were fitted with line-broadening parameters of signals from each phase constrained to be equal in order to improve the stability of the fits. This resulted in good fits. Figure 2b shows the fractions of indium in FeAl<sub>2</sub> (sum of site fractions associated with hyperfine parameters in Tab. 2) and FeAl (sum of the seven other site fractions). The phase boundary of FeAl and  $C_{seg}$  were determined from fitted solute fractions of the FeAl<sub>2</sub> phase. It was assumed that indium substituted at all Al sites in both phases, so that the value of  $A$  used in eq. 1 was accordingly 3/4. Furthermore, the phase boundary of FeAl<sub>2</sub> was assumed to be 33.3 at.% Fe. The result of fitting the data to Eq. 1 is shown by the curves in Fig. 2b, with values  $x_2=49.5(1)$  at.% Fe and  $C_{seg}=11.7(2)$ .

Reanalysis of data for Ni-Al phase mixtures. Data for the Ni<sub>2</sub>Al<sub>3</sub>-NiAl two-phase field have been reported [1,2] that show “enhancement” of the Ni<sub>2</sub>Al<sub>3</sub> signal. Ni<sub>2</sub>Al<sub>3</sub> has two inequivalent Al-sites with 2:1 ratio of sites per unit cell. In the earlier work, signals were erroneously interpreted as arising from indium solutes at both Al sites. However, from comparison with Ni<sub>2</sub>In<sub>3</sub> spectra it is now clear that indium only occupies the Al-site with 2 sites per unit cell in Ni-rich Ni<sub>2</sub>Al<sub>3</sub> [8,11]. Using the appropriate new value  $A=5/4$ , one obtains  $C_{seg}=2.3(3)$ .

Discussion. Segregation coefficients for indium solutes in the four systems studied are collected in Table 3, in which the magnitudes and directions of segregation of indium are indicated qualitatively. The range of coefficients can be seen to be quite large. Differences in energies of solutes in the two phases can be estimated from the segregation coefficients using an effective temperature that represents the lowest temperature at which solutes remained in equilibrium while cooling to room temperature. For example, using an effective temperature of ~450 °C leads to  $\Delta G \approx 0.24$  eV for  $C_{seg} \approx 45$ . Since  $\Delta G = \Delta H - T\Delta S$ , the energy difference arises from differences of enthalpies, vibrational entropies, or both. It can be seen that small enthalpy differences may produce large degrees of segregation. Alternatively, the segregation factor of 45 could be explained solely by an entropy difference of  $3.8 k_B$ . One way to distinguish between such enthalpy and entropy differences would be through equilibrium measurements at elevated temperature.

Table 3  
 Segregation coefficients of indium in different mixtures of compounds.

phase 1	segregation direction	phase 2	$C_{\text{seg}}$
PdGa	→	Pd <sub>5</sub> Ga <sub>3</sub>	0.6(2)
Ni <sub>2</sub> Al <sub>3</sub>	←	NiAl	2.3(3)
FeAl <sub>2</sub>	←	FeAl	11.7(2)
Pd <sub>3</sub> Ga <sub>7</sub>	←	PdGa	45(7)

The authors thank Slade Jokela for assistance with the experiments. This work was supported in part by the National Science Foundation under grants DMR 96-12306 and 00-91681.

1. Gary S. Collins, Luke S.-J. Peng and Matthew O. Zacate, *Z. Naturforschung* 55a (2000) 129.
2. Matthew O. Zacate, Gary S. Collins and Luke S.-J. Peng, *Mat. Sci. and Engin. A* (in press, 2001.)
3. Matthew O. Zacate, Bonner C. Walsh and Gary S. Collins, (to be published).
4. Luke S.-J. Peng (unpublished.)
5. Gary S. Collins, Steven L. Shropshire and Jiawen Fan, *Hyperfine Interactions* 62 (1990) 1.
6. A.R. Arends et al., *Hyperfine Interactions* 8 (1980) 191.
7. M Marszalek, B. Wodniecka, P. Wodniecki and A.Z. Hryniewicz, *Hyperfine Interactions* 80 (1993) 1029.
8. Matthew O. Zacate and Gary S. Collins, *Hyperfine Interactions* (this conference.)
9. M. Renteria et al., *Phys. Rev. B* 55 (1997) 14200; M. Renteria et al., *Z. Naturforschung* 55a (2000) 155.
10. Gary S. Collins, Luke S.-J. Peng and Mingzhong Wei, *Mat. Res. Soc. Symp. Proc.* 552 (1999) KK.4.2.1.
11. Matthew O. Zacate and Gary S. Collins (to be published).